Interaction of 8-Anilino-1-naphthalenesulfonate with Heptakis(2,3,6-tri-*O*-methyl)-β-cyclodextrin

Juziro NISHIJO,* Masako YASUDA, Mayumi NAGAI, and Makiko SUGIURA

Kobe Women's College of Pharmacy, Motoyama-kitamachi, Higashinada-ku, Kobe 658, Japan.
Received August 4, 1993; accepted November 29, 1993

The interaction of 8-anilino-1-naphthalenesulfonate (ANS) with heptakis(2,3,6-tri-*O*-methyl)-β-cyclodextrin (TOM-β-CD) was investigated in a 0.1 M phosphate buffer at pH 7.4 by fluorescence spectrophotometry. Utilizing the fact that the fluorescence intensity of ANS increases in the presence of TOM-β-CD, the thermodynamic parameters for inclusion complex formation were determined as follows: $\Delta G° = -8.95\,kJ \cdot mol^{-1}$ at 25 °C, $\Delta H° = -10.9\,kJ \cdot mol^{-1}$, $\Delta S° = -6.3\,J \cdot mol^{-1} \cdot K^{-1}$. The main driving force for the inclusion complex was considered to be the van der Waals–London dispersion forces, while the contribution of the hydrophobic interaction was small. Also, from the measurements of proton nuclear magnetic resonance spectra and studies with Corey Pauling Koltun models, the probable structure of the complex was determined. Further, the effects of permethylation on inclusion complex formation were discussed.

Keywords 8-anilino-1-naphthalenesulfonate; TOM-β-cyclodextrin; fluorescence; inclusion complex; thermodynamic parameter; ^{1}H-NMR

8-Anilino-1-naphthalenesulfonate (ANS) is known to be a fluorescence probe for exploring hydrophobic regions.[1] The fluorescence of ANS is quenched in water, but in hydrophobic environments, such as the cavity of cyclodextrin (CD), it is augmented substantially with shifts of the emission toward shorter wavelengths.[2] In previous papers, we have reported the interactions of ANS with α-,[3] β-,[4] and heptakis(2,6-di-*O*-methyl)-β-CD (DOM-β-CD)[5] in aqueous solution.

In the present study, the authors investigated the interaction between ANS and heptakis(2,3,6-tri-*O*-methyl)-β-CD (TOM-β-CD) by measuring changes in the fluorescence spectra of ANS in the presence of TOM-β-CD in a phosphate buffer to clarify the effect of permethylation. It is interesting to study the interaction between ANS and TOM-β-CD and to compare it with the results of other CD reported previously, because the macrocyclic ring TOM-β-CD is distorted by the steric hindrance caused by the methyl groups being introduced to hydroxyl groups.[6] The changes in enthalpy and entropy due to the formation of the inclusion complex were determined so that the driving force acting between the components of the inclusion complex could be clarified. Further, the probable structure of the inclusion complex was determined using Corey Pauling Koltun (CPK) models and considering proton nuclear magnetic resonance (^{1}H-NMR) data. No report concerning the interaction between ANS and TOM-β-CD has been found.

Experimental

Materials Reagent-grade TOM-β-CD, supplied by Nakalai Chemicals, Ltd., was recrystallized twice from water and dried for 10 h at 110 °C in a vacuum before use. Two kinds of ANS were supplied by Nakalai Chemicals, Ltd. For ^{1}H-NMR spectroscopy, ammonium salt recrystallized twice from water was used, and for other experiments, its magnesium salt purified by crystallization twice from water was used. The water used was obtained by twice distilling water purified with ion-exchange resin.

^{1}H- and ^{13}C-NMR Spectra ^{1}H- and ^{13}C-NMR spectra were taken on a Varian VXR-500 spectrometer with tetramethylsilane (TMS) as an external reference in deuterium oxide at 30 °C. Two-dimensional rotating frame nuclear Overhauser effect spectroscopy (ROESY) experiments were performed in the phase-sensitive mode methods using the State–Haberkorn method. Spectra were acquired with 256 t_1 increments and each increment consisted of 1 kilo data points from 16—32 transients. The spinlock mixing pulse of 400 ms was used. For the ^{1}H-detected heteronuclear multiple bond connectivity (HMBC) experiments, a preparation delay of $\pi = 60$ ms was used to the optimum evolution of heteronuclear long-range coupling.

Fluorescence Spectra Fluorescence spectra were measured with a Shimadzu RF-503A recording fluorescence spectrometer at 5, 15, 25, and 40 °C. To obtain a given temperature, water regulated at a constant temperature from a thermostat was circulated through the cell holder. The change of temperature during the measurements was within 0.1 °C. The lamp emission intensity changed only slightly during measurements. But in order to obtain reliable data, spectra were corrected by repeating the measurements of the standard sample after measurement of each sample.

Absorption Spectra Absorption spectra were taken on a Shimadzu UV 260 spectrophotometer at 25 °C. The measurements were carried out in a 0.1 M phosphate buffer of pH 7.4.

Results

Figure 1 shows the effects of TOM-β-CD on the absorption spectra of ANS. These spectra were measured using a buffer solution containing the same concentration of TOM-β-CD as the sample. The absorption at wavelengths longer than 350 nm, at which the isosbestic point was observed, increased. The changes in the absorption spectrum were similar to those found in β-CD and DOM-β-CD, though the hypochromic effects of TOM-β-CD at wavelengths of 217 and 265 nm were smaller than those of the latter two.

Figure 2 shows a part of the fluorescence spectra of 1.0×10^{-4} M of ANS measured in the presence of TOM-β-CD at concentrations of 1.0×10^{-3}—9.0×10^{-3} M in 0.1 M phosphate buffer (pH 7.4) at 25 °C. Fluorescence intensity increased as the concentration of TOM-β-CD increased with a shift of the fluorescence maximum to shorter wavelengths. These phenomena are the same as those reported in previous papers and, therefore, it is clear that interaction with TOM-β-CD is closely related to the cavity of the oligosaccaride.

As described above, the fluorescence intensity of ANS

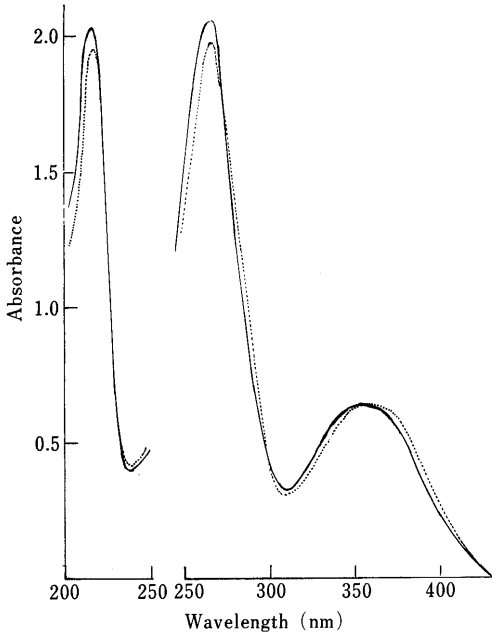

Fig. 1. Absorption Spectra of ANS in the Presence of TOM-β-CD in 0.1 M Phosphate Buffer, pH 7.4 at 25 °C

In the region of 200—250 nm: ——, ANS only (5.0×10^{-5} M); ------, ANS (5.0×10^{-5} M) + TOM-β-CD (1.0×10^{-2} M), in the region of 250—430 nm: ——, ANS only (1.3×10^{-4} M); ------, ANS (1.3×10^{-4} M) + TOM-β-CD (1.0×10^{-2} M).

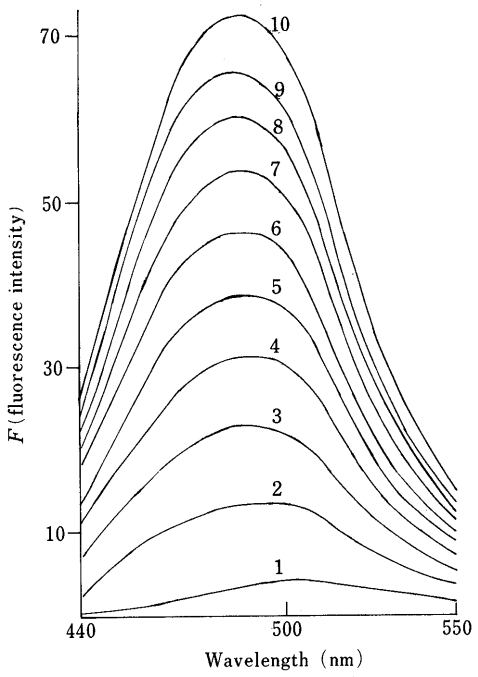

Fig. 2. Fluorescence Spectra of ANS (1.0×10^{-4} M) in the Presence of TOM-β-CD in 0.1 M Phosphate Buffer, pH 7.4 at 25 °C

TOM-β-CD concentrations (M) are as follows: 1, 0; 2, 1.0×10^{-3}; 3, 2.0×10^{-3}; 4, 3.0×10^{-3}; 5, 4.0×10^{-3}; 6, 5.0×10^{-3}; 7, 6.0×10^{-3}; 8, 7.0×10^{-3}; 9, 8.0×10^{-3}; 10, 9.0×10^{-3}. The excitation wavelength was 365 nm.

increases significantly in the presence of TOM-β-CD. By taking advantage of this effect of TOM-β-CD, the formation constant K of a 1 : 1 complex can be estimated from Eq. 1[3] using the nonlinear squares program MULTI,[7] in the same way as reported previously.

Table I. Thermodynamic Parameters for Inclusion Complex Formation of ANS with TOM-β-CD

Temp. (°C)	$K^{a)}$ (M^{-1})	$\Delta G°$ (kJ·mol^{-1})	$\Delta H°$ (kJ·mol^{-1})	$\Delta S°$ (J·mol^{-1}·K^{-1})
5	51.2	−9.10		
15	42.9	−9.01		
25	36.9	−8.95	−10.9±0.8	−6.3±0.8
40	30.2	−8.87		

a) These values are averages which were obtained from five repeat runs. Average probable errors are ±6% for K.

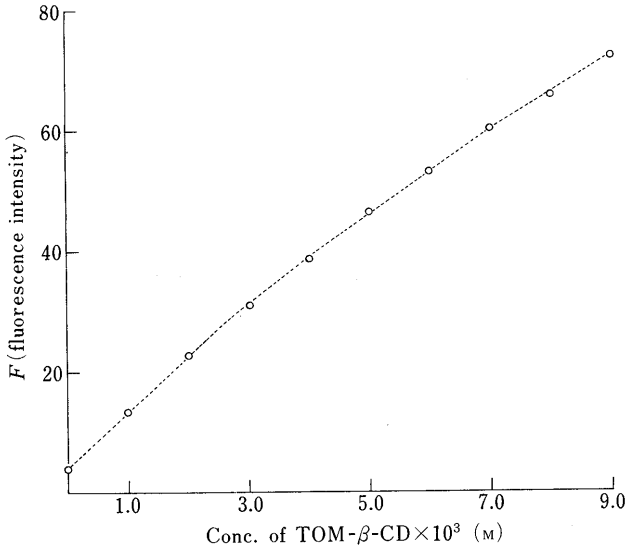

Fig. 3. Binding Curve of TOM-β-CD with ANS

○, observed fluorescence intensity; ----, theoretical curve, which was obtained from Eq. 1, using the calculated parameters.

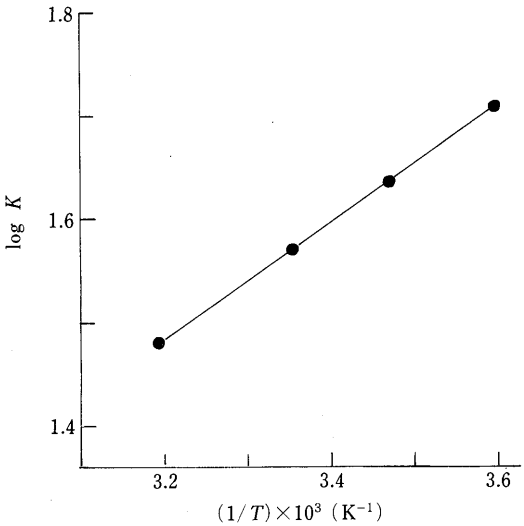

Fig. 4. The van't Hoff Plot of the Data in Table I

$$F=\frac{1}{1+C_oK}F_A-\frac{1}{1+C_oK}F_{\infty1:1}+F_{\infty1:1} \quad (1)$$

where F and C_o represent the fluorescence intensity observed and total concentration of ANS, respectively. Also, F_A and $F_{\infty1:1}$ denote the fluorescence intensity which should be observed when all ANS is free and when all

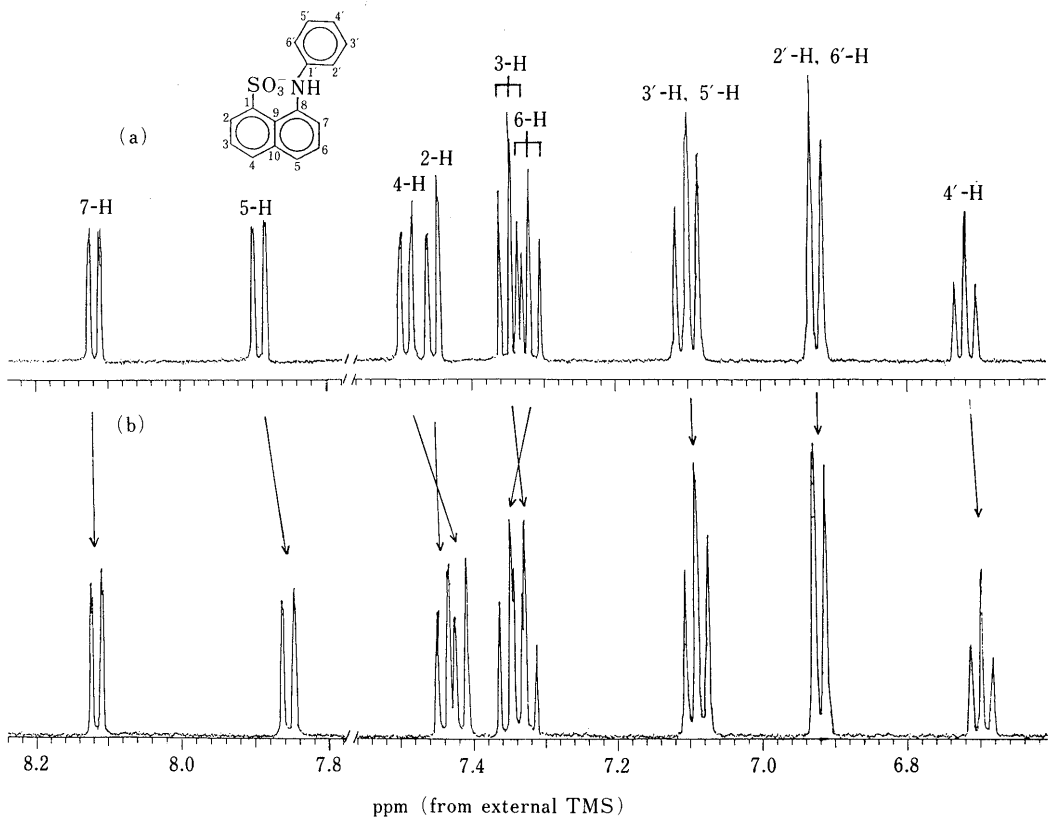

Fig. 5. ^{1}H-NMR Spectra of ANS in the Presence of TOM-β-CD in Deuterium Oxide at 30°C
(a) ANS alone (5.0×10^{-3} M), (b) ANS (5.0×10^{-3} M) + TOM-β-CD (1.5×10^{-2} M).

ANS has formed an ANS-TOM-β-CD complex, respectively. The values obtained at 5, 15, 25, and 40 °C are shown in Table I. Also, Fig. 3 shows the binding curve obtained using the calculated parameters. Figure 4 shows the van't Hoff plot of log K against the reciprocal of the absolute temperature. The changes in enthalpy ($\Delta H°$) and entropy ($\Delta S°$) accompanying the complexation, determined in the usual way, are shown in Table I.

^{1}H-NMR spectra and CPK models were used to estimate the structure of the inclusion complex between ANS and TOM-β-CD. In Fig. 5a, a ^{1}H-NMR spectrum of 5×10^{-3} M ANS in deuterium oxide at 30 °C is shown. The assignment of the proton signals of ANS has been reported.[3] The proton signals of ANS shifted with the addition of TOM-β-CD. In the presence of 1.5×10^{-2} M TOM-β-CD, for example, as shown in Fig. 5b, the proton signals of ANS shifted, but with accompanying no significant change in the shapes of the signals: the 6-H signals shifted downfield but the 7-H signal shifted only slightly, and the proton signals of the rest shifted upfield. In general, the signals due to the protons of the naphthalene ring shifted more than those of the benzene ring. At the naphthalene ring, the upfield shift of the signal due to 4-H was most prominent. At the benzene ring, the upfield shift of the 4′-H signal was most prominent, followed by 3′-H and 5′-H. Also, the magnitudes of the shifts of the ANS proton signals in the presence of TOM-β-CD at various concentrations are shown in Fig. 6.

A ^{1}H-NMR spectrum of 5.0×10^{-3} M TOM-β-CD solution is shown in Fig. 7a. The assignments of the proton signals of TOM-β-CD have already been carried out in

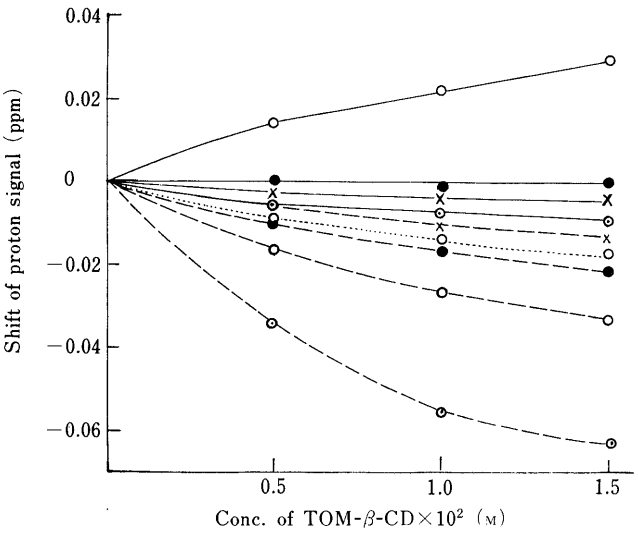

Fig. 6. Induced ^{1}H-NMR Chemical Shifts of ANS (5.0×10^{-3} M) in the Presence of TOM-β-CD
—○—, 6-H; —●—, 7-H; —×—, 2′-H, 6′-H; —⊙—, 3′-H, 5′-H; – – × – –, 2-H; – – ○ – –, 3-H; – – ● – –, 4′-H; – – ○ – –, 5-H; – – ⊙ – –, 4-H.

deuterated chloroform.[8] However, the spectrum obtained in deuterium oxide was not in agreement with the one in deuterated chloroform. Accordingly, the assignments of the proton signals were undertaken as follows; at first, the assignments of the proton signals of TOM-β-CD were undertaken using ^{1}H–^{1}H shift correlation spectroscopy (COSY), except for the proton signals of 5-H, 6-H and three methoxy groups. Then, ^{1}H–^{13}C COSY and the

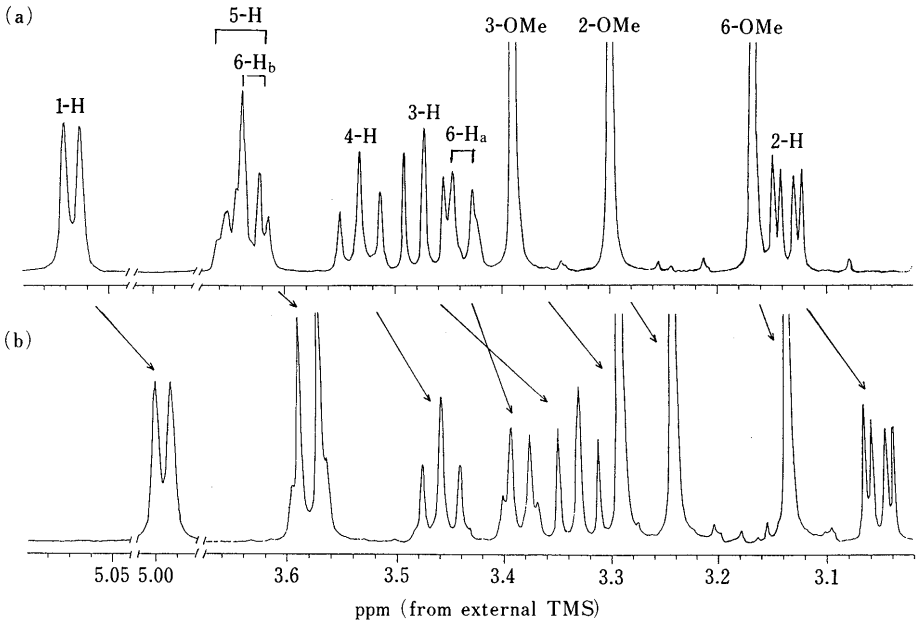

Fig. 7. ^{1}H-NMR Spectra of TOM-β-CD in the Presence of ANS in Deuterium Oxide at 30°C
(a) TOM-β-CD alone (5.0×10^{-3} M), (b) TOM-β-CD (5.0×10^{-3} M)+ANS (1.5×10^{-2} M).

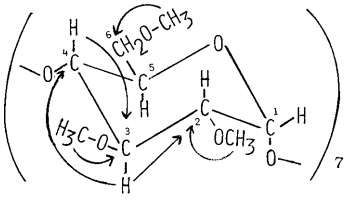

Fig. 8. ^{1}H–^{13}C Long Range Correlations in the HMBC Spectrum of TOM-β-CD

distortionless enhancement by polarization transfer (DEPT) method were used to assign the 5-H and 6-H signals. At the end of the assignments, an HMBC spectrum of TOM-β-CD was measured to assign the proton signals of the methoxy groups. In the HMBC spectrum, the long-range correlation between ^{1}H and ^{13}C, were observed as shown in Fig. 8. From the relationships of 2-OCH_3 → 2-C, 3-OCH_3 → 3-C, and 6-OCH_3 → 6-C, the assignment of the proton signals due to three methoxy groups were undertaken. The assignments determined in this way are shown in Fig. 7a.

^{1}H-NMR spectrum of TOM-β-CD shown in Fig. 7a is different from that in Fig. 7b in the presence of 1.5×10^{-2} M ANS. The comparison of these two spectra revealed that the signals due to the protons of all types in the TOM-β-CD shifted upfield remarkably in the presence of ANS. The shift of the signal due to 3-H on the inner surface of the cavity on the side of methylated secondary hydroxyl group was most prominent, followed by the signals due to 3-OCH_3 and 2-H, in this order. On the other hand, the upfield shift of the signal due to 6-OCH_3 lying on the side of the methylated primary hydroxyl group was smallest, followed by the signals due to 6-H and 5-H lying on the side of methylated primary hydroxyl group. The magnitudes of the shifts of the proton signals due to TOM-β-CD in the presence of ANS at various concentrations are shown in Fig. 9.

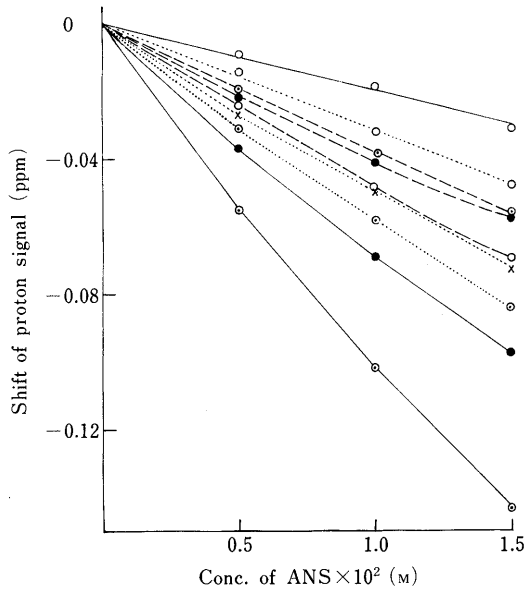

Fig. 9. Induced ^{1}H-NMR Chemical Shifts of TOM-β-CD (5.0×10^{-3} M) in the Presence of ANS
—○—, 6-OMe; ---○---, 6-H_a, 6-H_b; --⊙--, 5-H; --●--, 2-OMe; --○--, 1-H; ---×---, 4-H; ---⊙---, 2-H; —●—, 3-OMe; —⊙—, 3-H.

Three of possible structures of the inclusion complex, judging from the investigation using CPK models, are described below (Fig. 10): (a) ANS is enclosed in the cavity of TOM-β-CD from the methylated secondary hydroxyl group side at the head of benzene ring. The whole benzene ring and about 65% of the naphthalene ring containing a $-SO_3^-$ group are included; (b) only the naphthalene ring is enclosed from the side of the methylated secondary hydroxyl group, the benzene ring being left outside the cavity; or (c), the benzene ring is mainly enclosed from the side of the methylated primary hydroxyl group, the naphthalene ring being left outside the cavity. It is

considered that upfield shifts of the proton signals lying on the inner surface of TOM-β-CD result mainly from the magnetic anisotropy of either the benzene or naphthalene ring of the ANS molecule. Therefore, the result that the magnitudes of the upfield shifts of the signals due to the protons on the inner surface of TOM-β-CD are in the order of 3-H > 5-H > 6-H suggests that the structure shown in Fig. 10c cannot occur. In the structure described in Fig. 10a, it may be assumed that the 5-H and 3-H signals of TOM-β-CD show an upfield shift to a nearly similar extent. However, the upfield shift of the 3-H signal was more significant than that of 5-H. Therefore, it seems unlikely that the complex structure in Fig. 10a is preferential.

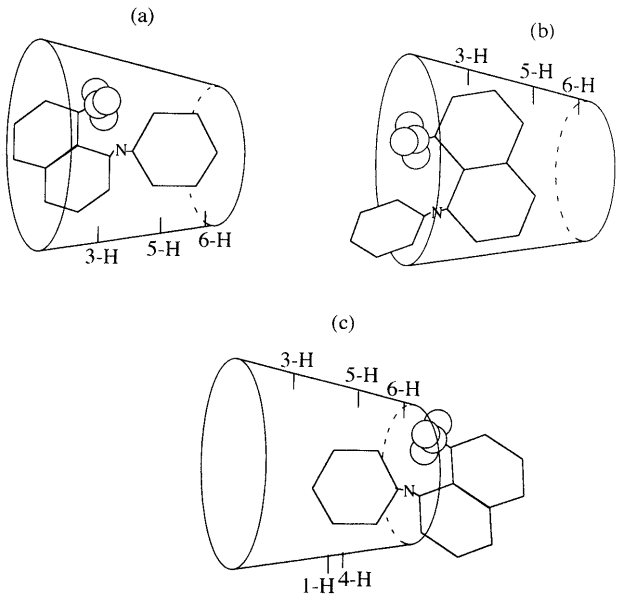

Fig. 10. Possible Structures of the Inclusion Complex of ANS with TOM-β-CD in Aqueous Solution Based on CPK Space-Filling Models

If the complex has the structure described in Fig. 10b, it would not be surprising for the upfield shift of the 3-H signal to be greater than that of 5-H, or for that of 5-H to be greater than that of 6-H. Therefore, from the induced chemical shifts by complexation it was assumed that the structure described in Fig. 10b is most preferential regarding the complex between ANS and TOM-β-CD.

To confirm the structure of the inclusion complex, ROESY spectra were measured. In a ROESY spectrum of the solution containing ANS (5.0×10^{-3} M) and TOM-β-CD (5.0×10^{-3} M), cross peaks connecting the 5-H of TOM-β-CD to the benzene protons of ANS, except 4′-H, were observed. Therefore, it is certain that the benzene ring of ANS is enclosed deeply in the cavity of TOM-β-CD from the side of the methylated secondary hydroxyl group, as shown in Fig. 10a. Also, cross peaks connecting the 5-H of TOM-β-CD to the 6-H of ANS were observed. Further, in a ROESY spectrum of the solution containing ANS (1.0×10^{-2} M) and TOM-β-CD (5.0×10^{-3} M), a cross peak was observed between 4-H of ANS and 5-H of TOM-β-CD, in addition to the cross peaks observed in a molar ratio of 1 : 1 (Fig. 11). Therefore, it is clear that the naphthalene ring of ANS is enclosed in the cavity of TOM-β-CD. It was presumed that the structure shown in Fig. 10b was preferential according to the induced chemical shifts. But, considering that the ROESY spectra gives direct information, it is reasonable to conclude that the structure shown in Fig. 10a exists to too small extent.

Discussion

If the structure shown in Fig. 10a exists even to a small extent, the upfield shift of the 5-H of TOM-β-CD seems too small. However, this may be because the 5-H of TOM-β-CD comes into contact with the naphthalene ring of ANS, which is inclined in the cavity as shown in Fig.

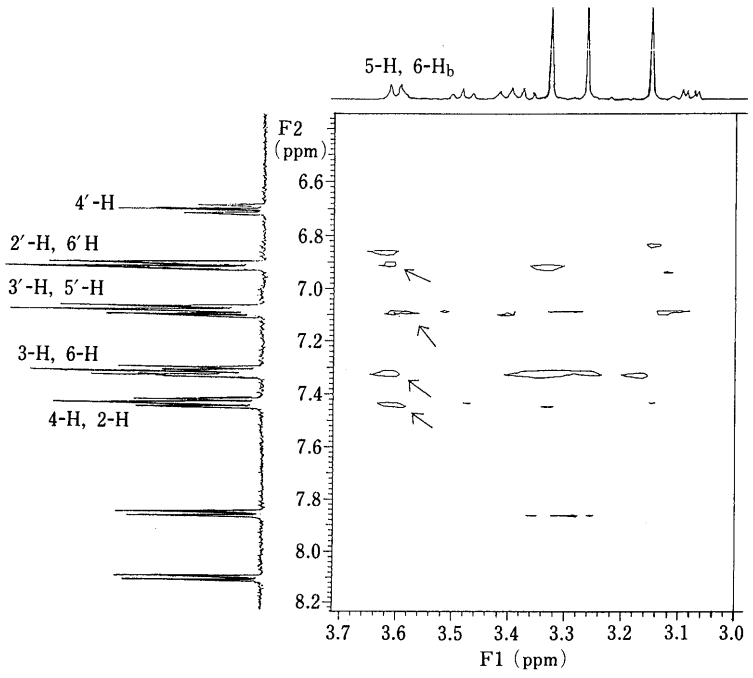

Fig. 11. ROESY Spectrum of Solution Containing ANS (1.0×10^{-2} M) and TOM-β-CD (5.0×10^{-3} M)

10b, and therefore, the upfield shift of the 5-H signal is compensated for by the steric compression effect, bringing about the downfield shift.[9]

It has been known that[4,5] signals due to the protons which do not come into close contact with the atoms on the inner surface of CD tend to shift upfield by the C–C bond anisotropy effect, and so on.[10] If the complex has the structure shown in Fig. 10a, in which the benzene ring is relatively loosely included, it is expected that the protons due to the benzene ring shift upfield and the results obtained in Fig. 6 support the existence of the structure shown in Fig. 10a. Also, the upfield shift of the 4′-H signal was most prominent in those of benzene protons. This suggests that 4′-H exists nearer to the center of the cavity, as shown in Fig. 10a, in which 4′-H has less tendency to come into contact with atoms on the inner surface of TOM-β-CD.

Next, the structure shown in Fig. 10b will be discussed from the standpoint of the induced chemical shifts of ANS protons in the presence of TOM-β-CD (Fig. 6). In Fig. 10b, 4-H and 5-H of the naphthalene ring exist in the cavity without close contact with the atoms on the inner surface of the host molecule. This might induce prominent upfield shifts of the signals due to 4-H and 5-H. Also in Fig. 10b, the 6-H of ANS tends to come into close contact with the neighborhood of the 5-H of TOM-β-CD. Therefore, it was assumed that the prominent downfield shift of 6-H resulted from the contact, namely, the steric compression effect.[9] Further, the upfield shift of the 4-H signal of ANS was more significant than that of the 5-H of ANS. This may be because the 4-H exists nearer to the inner surface of the cavity than the 5-H, which would make it more subject to a C–C bond anisotropy effect. Therefore, the minor axis of the naphthalene ring is slightly inclined to the axis of the cavity, as shown in Fig. 10b. Also, the upfield shifts of the 3-H and 2-H signals of ANS were small. It may be because the upfield shift of 3-H may be compensated for by the steric compression effect due to the contact with the neighborhood of 3-H on the inner surface of TOM-β-CD, and because 2-H exists in the neighborhood of the entrance of the cavity, the influence due to complexation being weak.

In the case of complexation in aqueous solution, the various driving forces have been reported to play a big part in the interaction.[11] However, according to Tabushi *et al.*, the van der Waals–London dispersion forces and hydrophobic interaction are major driving forces for the inclusion complexation between cyclodextrin and a guest molecule.[12] In the present study, it was found that the complexation was accompanied by negative changes in both enthalpy and entropy, though the change in entropy was small. These thermodynamic parameters suggest that the van der Waals–London dispersion forces are mainly responsible, whereas hydrophobic interaction is only a minor contributor to inclusion complex formation. Thermodynamic parameters for inclusion complex formation between ANS and cyclodextrin have already been determined,[4,5] and are shown in Table II for comparison. At 25 °C, the formation constant K for β-CD is greatest, followed by DOM-β-CD and TOM-β-CD in this order. The further methylation proceeds, the greater the decrease in the formation constant K. In contrast to the fact that the benzene ring of ANS is mainly included in the complex of ANS-β-CD, the benzene ring and almost all of the naphthalene ring containing a $-SO_3^-$ group are included in the complex of ANS-DOM-β-CD, resulting in a larger decrease in entropy change with the larger decrease in enthalpy change. As a result, the formation constant K for DOM-β-CD may be smaller than that for β-CD.

Table II. Thermodynamic Parameters for Inclusion Complex Formation of ANS with β-CD and DOM-β-CD

	K (25 °C) (M^{-1})	ΔH° ($kJ \cdot mol^{-1}$)	ΔS° ($J \cdot mol^{-1} \cdot K^{-1}$)
β-CD	70.9	-7.9 ± 0.8	8.8 ± 0.8
DOM-β-CD	63.2	-13.4 ± 1.3	-10.9 ± 1.3

In the present study, concerning TOM-β-CD, it has been reported that the macrocyclic ring is remarkably distorted from a regular heptagonal structure and has a wider cavity on the side of the methylated secondary hydroxyl group, though the entrance to the cavity on the methylated primary hydroxyl group becomes more narrow.[6] Also, TOM-β-CD has the same deep cavity as DOM-β-CD, the cavity of which is deeper than that of β-CD. These structural changes can be confirmed by the model built with CPK models. Therefore, when ANS is included as shown in Fig. 10a, more space than in the case of DOM-β-CD exists between the molecules of ANS and TOM-β-CD, and unfortunately, the $-SO_3^-$ group enters into the hydrophobic cavity. Also, in Fig. 10b, additional space exists between both molecules, though the terminal atoms along the apsis of the naphthalene ring tend to come into contact with those on the inner surface of TOM-β-CD, as mentioned above. Consequently, it seems valid that the formation constant K for TOM-β-CD is the smallest of those of the three CD.

From the discussion carried out above, it is reasonable that enthalpy change for the complex formation of ANS-TOM-β-CD is less negative than that of ANS-DOM-β-CD, since ANS in the complex of ANS-TOM-β-CD is not wholly included, as in the complex of DOM-β-CD, but is more negative than that of the complex of ANS-β-CD since the ANS in that complex has a larger area of contact with TOM-β-CD than with β-CD in the complex of ANS-β-CD. Also, it is reasonable that the entropy change for the complex formation of ANS-TOM-β-CD is negative in contrast to a positive value for the ANS-β-CD complex because ANS in the complex of ANS-TOM-β-CD is included more deeply and more tightly than in the complex of ANS-β-CD. Also, it can be presumed that the release of water from the inside of the cavity of β-CD might contribute to the positive entropy change, to some extent, in the complex formation of ANS-β-CD.[13] Further, it is reasonable that entropy change for the complex formation of ANS-TOM-β-CD is less negative than that of ANS-DOM-β-CD because ANS in the complex of ANS-TOM-β-CD is not included as tightly as it is in the complex of ANS-DOM-β-CD.

References

1) D. C. Turner, L. Brand, *Biochemistry*, **7**, 3381 (1968).
2) G. R. Penzer, *Eur. J. Biochem.*, **25**, 218 (1972).
3) J. Nishijo, M. Yasuda, M. Nagai, *Chem. Pharm. Bull.*, **39**, 5 (1991).
4) J. Nishijo, M. Nagai, *J. Pharm. Sci.*, **80**, 58 (1991).
5) J. Nishijo, M. Nagai, M. Yasuda, *Carbohydr. Res.*, **245**, 43 (1993).
6) K. Harata, K. Uekama, M. Otagiri, F. Hirayama, *Bull. Chem. Soc. Jpn.*, **56**, 1732 (1983).
7) K. Yamaoka, Nakagawa, *J. Pharmacobio-Dyn.*, **6**, 595 (1983).
8) J. R. Johnson, N. Shankland, I. H. Sadler, *Tetrahedron*, **41**, 3147 (1985).
9) D. J. Wood, F. E. Hruska, W. Saenger, *J. Am. Chem. Soc.*, **99**, 1735 (1977).
10) T. Nakajima, M. Sunagawa, T. Hirihashi, K. Fujioka, *Chem. Pharm. Bull.*, **32**, 384 (1984).
11) M. Komiyama, M. L. Bender, *J. Am. Chem. Soc.*, **100**, 2259 (1978).
12) I. Tabushi, Y. Kiyosuke, T. Sugimoto, K. Yamamura, *J. Am. Chem. Soc.*, **100**, 926 (1978).
13) K. Linder, W. Saenger, *Angew. Chem. Int. Ed. Engl.*, **17**, 694 (1978).